



Wear evolution of pyramid-structured abrasive belts and its effect on grinding operations

Yingjie Liu², Wenxi Wang¹, Jing Zhao², Yuanhanxu Song³ & Lai Zou¹

¹State Key Laboratory of Mechanical Transmission for Advanced Equipment, Chongqing University, No. 174, Shazhengjie Street, Shapingba, Chongqing, 400044, China.

²College of Mechanical and Vehicle Engineering, Chongqing University, No. 174, Shazhengjie Street, Shapingba, Chongqing, 400044, China.

³Undergraduate School of Chongqing University, Chongqing University, No. 174, Shazhengjie Street, Shapingba, Chongqing, 400044, China.

Abstract

Pyramid-structured abrasive belts are commonly used in the precision processing of free-form surfaces due to their exceptional cutting performance and service life. However, the unavoidable abrasive belt wear significantly impairs its grinding performance. In order to promote its further application in the field of intelligent manufacturing, this paper investigates the wear evolution law of a pyramid-structured abrasive belt based on the full-lifecycle grinding experiments, detects the surface morphology of the abrasive belt and the workpiece, and also solves the time-domain and frequency-domain features of the collected grinding force and sound signals. The results show that the main form of wear on pyramid-structured abrasive belts is abrasive wear, which is also accompanied by adhesive wear. At the beginning of belt wear, both the belt wear rate and the material removal rate were at a high and fluctuating level, decreasing rapidly and then slowly to 0 g/s as the grinding time increased. The machining performance of the pyramid-structured abrasive belts is more stable, with the machined surface roughness values of R_a stabilized at 0.4 - 0.5 μm and S_a stabilized at 0.1 - 0.2 μm until the belt lost its surface polishing ability. It was also found that the time-domain features of the grinding force and sound signals exhibited a strong correlation with the wear state of the abrasive belts.

Keywords: Pyramid-structured abrasive belt, Wear evolution, Surface processing quality, Grinding process signal.

1. Introduction

With the rapid development of intelligent manufacturing technology, precision machining technology [1] plays an increasingly important role in industrial production. Especially in the aviation, automotive, and other manufacturing industries [2], the efficient and precise machining of complex free-form surfaces is a key link to improve product performance and production efficiency [3]. As an advanced abrasive tool, the pyramid-structured abrasive belt has become a major research object in the field of precision machining due to its unique stacked pyramid-structured cell design, which shows excellent cutting performance and long service life.

However, the performance of any abrasive tool is inevitably affected by wear [4,5], and the wear problem of abrasive belts is particularly prominent. Wear not only affects the use efficiency and life of the abrasive belt itself but also directly affects the processing quality and safety [6]. Therefore, an in-depth study of the wear of abrasive belts and their impact on machining performance is the key to promoting the progress of this technology and realizing its wider application in intelligent manufacturing [3].

The issue of abrasive belt wear has been a topic of significant interest within the field [7,8]. Xiao

and Huang [9] developed a full-lifecycle material removal model and found that the material removal rate decreases in stages with abrasive belt wear and is accompanied by an unstable rate of change rather than a simple linear relationship. Mezghani et al. [10] proved through numerous experiments that the machining quality of the workpiece surface depends on the wear state of the abrasive belts. Wang et al. [11] carried out a comprehensive study on the wear evolution of abrasive belts and found that the surface roughness varies with the wear of abrasive grits, even under the same grinding parameters. He et al. [12] investigated the critical transition conditions and identification methods between different grinding modes of ceramic abrasive belts and found that the abrasive belt wear is closely related to the parameters. Serpin et al. [13,14] carried out a comparative analysis of new-generation abrasive belts with four abrasive grain morphologies such as pyramidal structure and multiscale characterization of their abrasive belt wear and found that the arrangement of the cytosol of the pyramid-structured abrasive belts resulted in better durability. Zaborski et al. [15] found that the grinding performance of pyramid-structured abrasive belts is more excellent and stable. The above study provides a reference point for further research into the wear evolution of pyramidal abrasive belts and its effect on the grinding process.

This paper systematically analyses the wear evolution law of abrasive belts and its influence on the grinding performance using full life cycle grinding experiments of pyramid-structured abrasive belts. The rate of wear and material removal of the abrasive belts was quantified, and the surfaces of the belts and workpieces were examined. Additionally, the relationship between dynamic monitoring indicators, such as grinding force and sound signals, and the wear state of the abrasive belts was investigated. The study aims to provide a scientific basis and technical support for the optimal design of pyramid-structured abrasive belts and their application in complex free-form surface machining.

2. Materials and Methods

In this study, the degree of abrasion of abrasive belts will be quantitatively evaluated by the percentage of abrasive belt wear mass[16].

The experiments were carried out on a robotic flexible belt grinding system, which mainly consists of an industrial robot, an active contact flange, and a belt drive device, as shown in Figure 1 (a). A Fanuc six-axis robot (M710 iC-50) with a repeat positioning accuracy of 0.03 mm was used to complete the grinding trajectory operation, and an active contact flange (FERROBOTICS ACF/111/04HD) was used to realize the real-time control of the grinding normal force. The KUNWEI KWR75B force sensor with an accuracy of 0.1 N is installed on the robot's end-effector for the acquisition of real-time grinding force, and the sound signal is measured by the self-constructed sound sensor (the combination of the Aiwa microphone AWA14423 and the preamplifier AWA14604) and converted into samples by the digital acquisition card YE6231C (accuracy $\pm 0.5\%$), as shown in Figure 1 (b). The processing material used for the experiment was TC4 [17], with a cutting size of 150 mm \times 100 mm \times 3.5 mm. The abrasive belt was a pyramid-structured abrasive belt produced by 3M Company of the U.S.A., with a size of 3480 mm \times 10 mm. The process parameters of the experiment are shown in Table 1. The workpieces and abrasive belts were removed after each grinding cycle and weighed separately using an electronic balance with an accuracy of 0.001 g to obtain the corresponding abrasive belt wear quality and material removal during that grinding cycle.

Table 1 - Experiment process parameters.

Items	Index
Abrasive belt model	3M Trizact 237AA
Grit size	A6
Workpiece material	TC4
Grinding speed, v_s	15 m/s
Grinding speed, v_w	0.5 mm/s
Normal grinding force	10 N

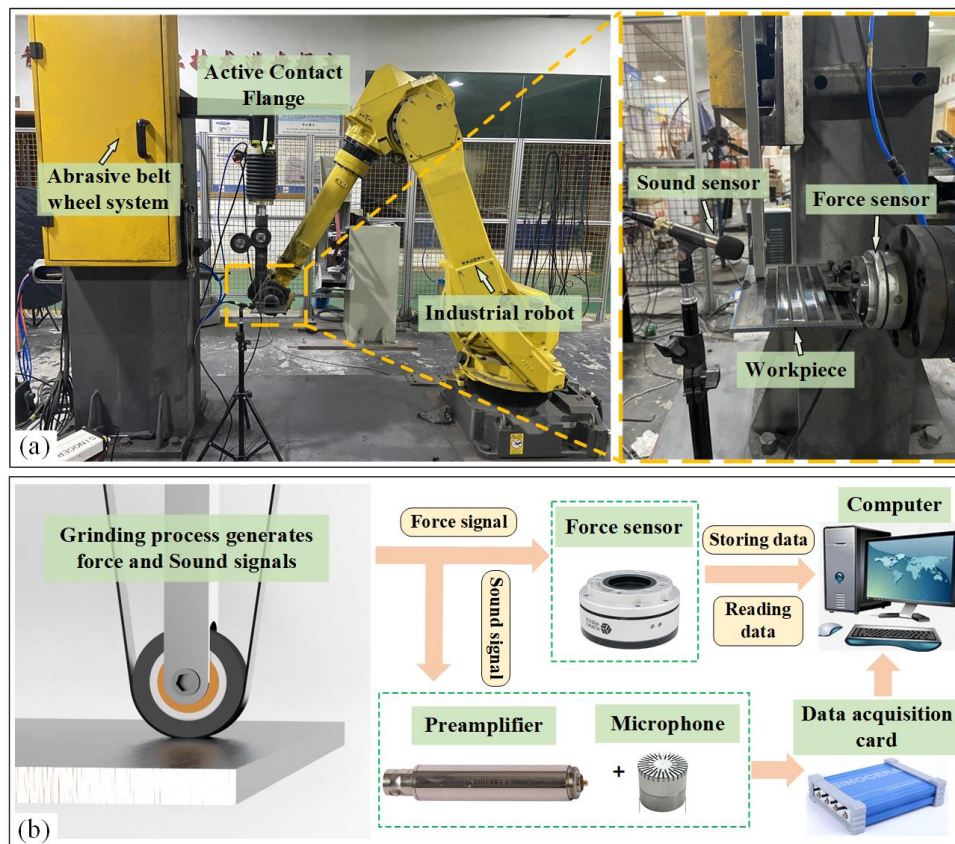


Figure 1 – (a) Robotic flexible belt grinding system, (b) signal acquisition equipment.

3. Results and Discussion

3.1 Abrasive Belt Wear

3.1.1 Abrasive Belt Wear Form

Figure 2 shows the change in surface morphology of a pyramid-structured abrasive belt over its full life cycle as captured by an industrial microscope. It can be seen that abrasion wear is the main form of wear for pyramid-structured abrasive belts. Abrasive wear is caused by repeated friction between the abrasive cell and the workpiece, which gradually blunts the apex of the cell into a small flat surface, as shown in Figure 2 (b). In this process, a larger flat surface is formed at the tip of the cell, which affects the cutting efficiency of the abrasive belt.

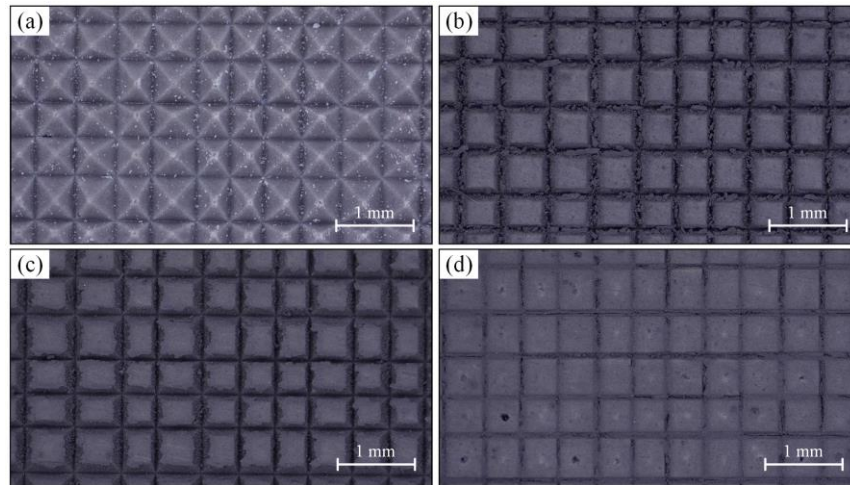


Figure 2 – Evolution of surface morphology of abrasive belts: (a) unworn, (b) initial wear, (c) middle wear, (d) terminal wear.

The elemental composition and distribution on the abrasive grain surface at different wear stages were detected by energy dispersive spectrometer (Figure 3). It can be found that Ti, V, and O elements are widely distributed on the abrasive grain surface, which indicates that the pyramid-structured abrasive belts have adhesive wear at the same time. In addition, the elements of Ti, V, and O always appear in the same position, indicating that the material adhered to is a titanium alloy workpiece. This is because a large number of chips are generated during the grinding process, especially under high temperatures and high pressure, and these chips are easy to adhere to the abrasive surface and remain in the chip holding space between the abrasives. In addition, as the abrasive belt wears, the content of Ti, V, and O elements on the abraded abrasive grains rises, indicating that the abrasive grains become stronger in the late stage of abrasion by adhesive wear. Since adhesive wear dulls the abrasive grains, thus reducing their cutting ability; in this case, the abrasive grains are easily dislodged and the surface of the workpiece may be burned. In the actual manufacturing process, adhesive wear should be avoided.

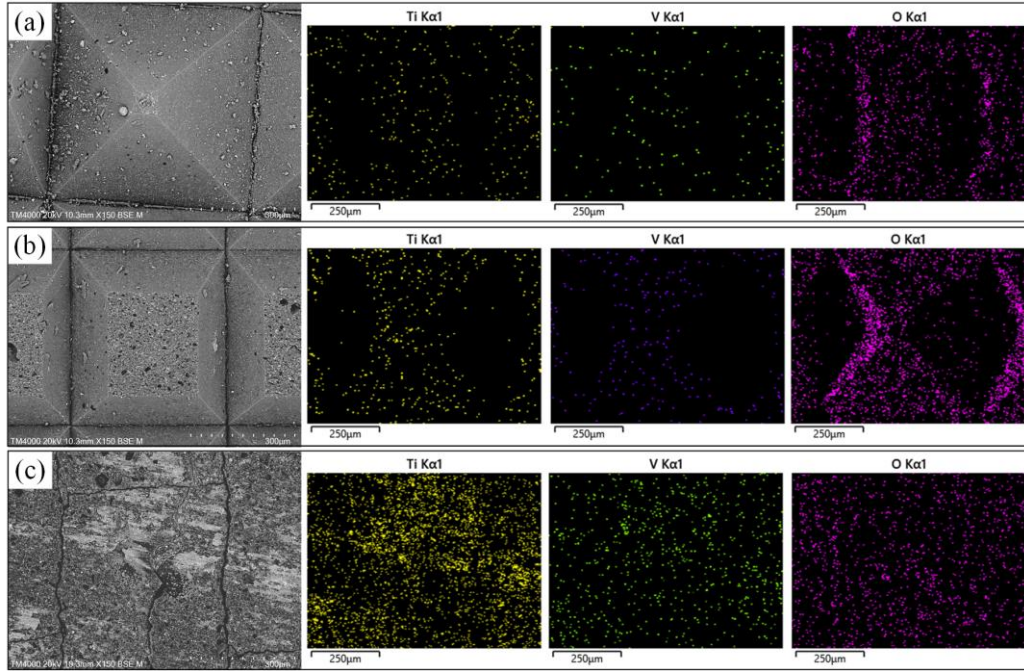


Figure 3 - EDS spectra of worn abrasive grain: (a) initial wear, (b) middle wear, (c) terminal wear. At the same time, it was found that the pyramid-structured cell had an overall fracture in the early stage of wear, and the possible reasons were analyzed because of the internal stresses. The stresses generated in the internal material when the cell is subjected to grinding are shown in Figure 4. f_n and f_t are the normal and tangential forces on the cell from the surface of the workpiece, respectively, and the direction and magnitude of the stresses in the plane at a depth of h are shown in Figure 4, with σ_t being the shear stress in the horizontal direction and σ_n the tensile and compressive stresses in the vertical direction.

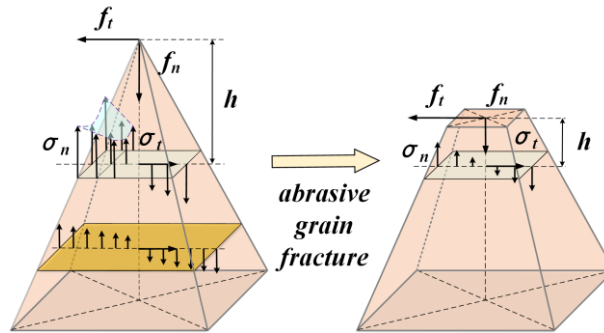


Figure 4 - Schematic diagram of the overall fracture of the abrasive cell.

3.1.2 Abrasive Belt Material Removal

Figure 5 (a) shows the evolution of the cumulative wear mass and wear rate of the pyramid-structured abrasive belts over the entire life cycle. The initial stage of belt wear is characterized by a rapid increase in the cumulative wear mass and a high and fluctuating wear rate, which gradually slows down as the grinding time increases and the belt wear rate decreases close to zero.

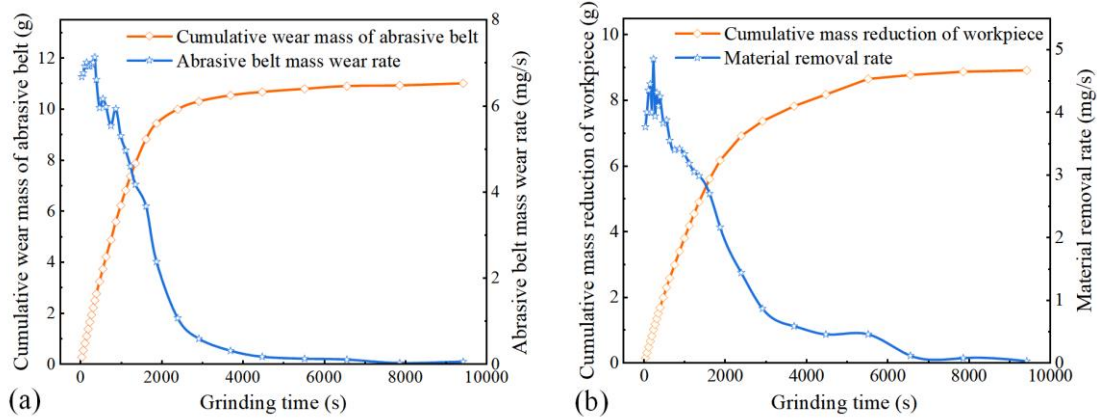


Figure 5 - (a) belt cumulative wear loss and mass wear rate, (b) TC4 cumulative mass reduction and belt material removal rate.

This phenomenon may be related to the more prominent pyramidal cells on the surface of the abrasive belts, which have a higher cutting capacity under the localized high pressure at the beginning of the wear phase, contributing to a more efficient removal of material from the surface of the workpiece. However, it is also these cells that have higher internal stresses and are prone to fracture, which causes a sharp decline in the overall quality of the belt in the pre-grinding stage. As grinding time progresses, the pyramidal structure of the cells on the surface of the abrasive belt undergoes abrasion, fracture, or forms a layer of grinding product that adheres to the surface of the abrasive belt. This may result in a slowing of the overall wear rate of the abrasive belt as the grinding process gradually stabilizes and the changes in the abrasive belt surface are relatively uniform and no longer show the initial sharp decline.

Figure 5 (b) shows the evolution of the cumulative mass reduction of the workpiece and the material removal rate of the abrasive belt during the whole life cycle. In the early stage of wear, the abrasive belt shows high material removal capability, and as the abrasive belt wears, this capability gradually decreases and stabilizes, and finally decreases to 0, which indicates that the abrasive belt has lost its material removal capability at this time. This is mainly because, in the early stage of wear, the pyramid-structured cell tip plane is small, the number of abrasive grains microcrystalline in contact with the workpiece is small, and in the same grinding normal force, abrasive grains microcrystalline cutting ability is stronger. In addition, this phenomenon may also be related to the more prominent surface of the cell, in the early stage of wear belt local high-pressure action, the height of the cell is easy to cut into the workpiece, resulting in macroscopic cutting behavior. For these reasons, the material removal rate is at a high level in the early stages of belt wear. With the abrasive belt wear, the unevenness of the surface of the abrasive belt is weakened, so that the material removal rate of the abrasive belt gradually slows down and eventually stabilizes.

3.2 Surface Processing Quality

Figure 6 shows the evolution of the surface roughness values R_a and S_a of the machined workpiece after grinding. At the beginning of belt wear, R_a and S_a are relatively high but show a decreasing trend. In the middle stage of belt wear, R_a and S_a remain stable, which shows that the grinding performance of the pyramid-structured abrasive belts is more stable and excellent.

At the end of the belt wear period, the R_a and S_a values gradually increase and approach the initial roughness values of the machined surface. As the pyramid-structured abrasive belts wear, the roughness of the machined surface tends to decrease for a short period, then remains stable for a long period, and then rises to the initial value when the abrasive belts lose the ability to polish the surface.

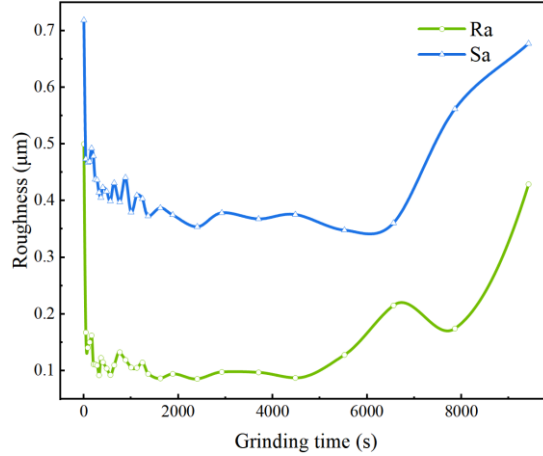


Figure 6 - Roughness values of the workpiece surface

This may be because in the early stage of wear, the height of the pyramid-structured cell is uneven, and there is an overall fracture phenomenon, the grinding process is not stable, so the roughness value of the processed surface at this time is slightly higher. With the gradual wear of the abrasive belt, the height of the cell body is gradually consistent, and the top plane increases [18], the number of abrasive grains involved in grinding increases, the grinding normal force on individual abrasive grains decreases, and the grinding process is more stable, resulting in a more stable and smaller processing roughness value.

3.3 Grinding Process Signals

3.3.1 Grinding Force Signals

The Root Mean Square (RMS) is a measure of the average strength of a signal in the time domain, reflecting the effective value of the signal's energy. The RMS provides a statistical average of the signal's amplitude and is widely used in engineering and physics to quantify the strength of a signal. The formula for solving the RMS of the grinding force is:

$$RMS = \sqrt{\frac{1}{T} \int_0^T [F(t)]^2 dt} \quad (1)$$

Where T is the market of the acquired signal and $F(t)$ is the corresponding grinding force. The evolution of the root mean square values of tangential and normal forces over the full life cycle of the abrasive belt is shown in Figure 7.

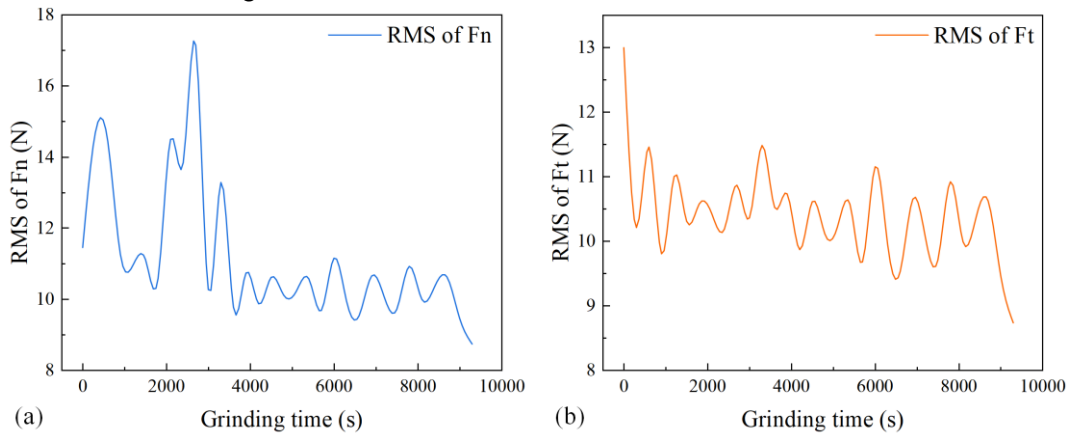


Figure 7 – Time domain features of grinding force signal: (a) RMS of normal force, (b) RMS of tangential force.

In the early stage of abrasive belt wear, the RMS of normal force and tangential force are at a high level, with the gradual abrasion of the abrasive belt, the RMS value of normal force gradually

decreases to fluctuate around the stabilized value, and the fluctuation of the RMS value of tangential force is still a decreasing trend, which may be related to the gradual decrease of the material removal ability of the abrasive belt.

3.3.2 Grinding Sound Signals

The composition of the experimentally captured sound signal is shown in Figure 8. To study the variation of the grinding sound signal over the full life cycle of a pyramid-structured abrasive belt, it should be appropriately processed to minimize the interference of noise [19].

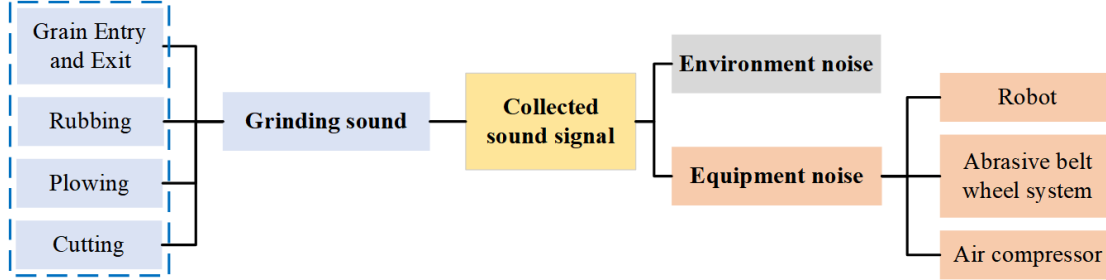


Figure 8 - Acquisition of sound signal sources.

Wavelet Packet Decomposition (WPD) [20] is a signal processing technique that provides finer spectral analysis by refining the frequency information through recursive decomposition. It is commonly used for signal denoising and feature extraction. The frequency and time domain signals of each frequency band of the ground sound signal after two-layer wavelet packet decomposition are shown in Figure 9. It can be seen that in the AD2 and DD2 frequency bands, the ambient sound is more differentiated from the grinding sound, which can better study the evolution of the sound signal in the wear process.

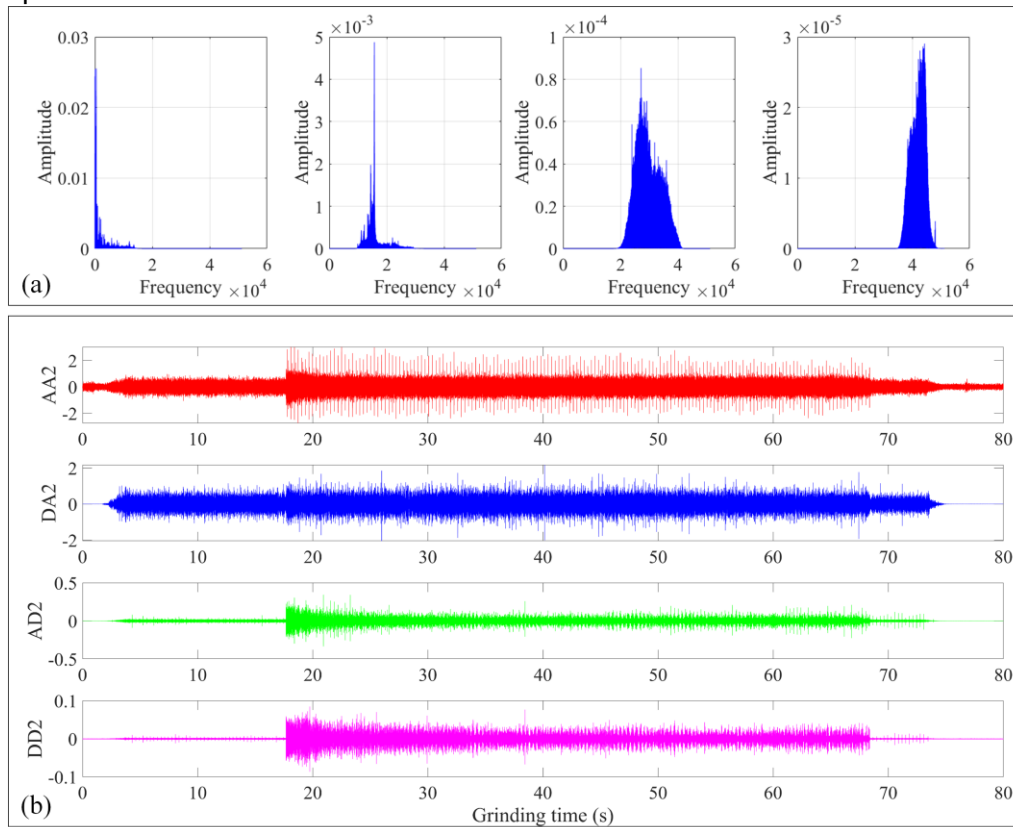


Figure 9 – Sound signal after wavelet packet decomposition processing: (a) frequency domain, (b) time domain.

The form factor (FF) is used to describe the smoothness of the signal waveform, and the margin

index (MI) is used to describe the sharpness and concentration of the signal after the wavelet packet processing of every 0.1 s of the sound signal is solved for the time domain and frequency domain features. The formulas for the waveform factor and margin index are as follows:

$$FF = \frac{\sqrt{\frac{1}{N} \sum_{i=1}^N A_i^2}}{\frac{1}{N} \sum_{i=1}^N |A_i|} \quad (2)$$

$$MI = \frac{\max(|A|)}{(\frac{1}{N} \sum_{i=1}^N |A_i| - \frac{1}{N} \sum_{i=1}^N A_i)^3} \quad (3)$$

where A_i is the acquired sound signal and N is the signal length. The evolution of the RMS, FF, and MI of the grinding sound signal is shown in Figure. 10. The RMS value of the sound signal is higher at the beginning of the abrasive belt wear, decreases as the abrasive belt wear increases, and is more stable in the middle and late stages of the abrasive belt wear. The FF of the signal fluctuates greatly at the beginning of the abrasive belt wear and gradually decreases in the middle and late stages. The signal's MI, on the other hand, continues to rise throughout the process.

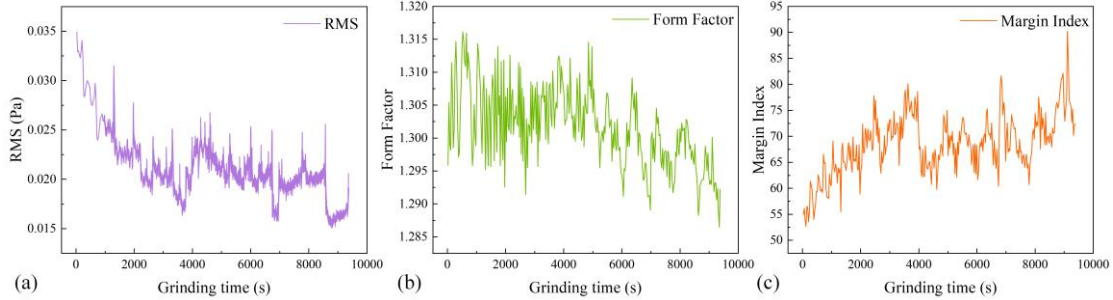


Figure 10 - Time domain features of grinding sound signal: (a) RMS, (b) Form Factor, (c) Margin Index.

It is analyzed that in the early stage of wear, the height of the pyramidal structural cytosol is higher and uneven, and the cutting ability is higher, accompanied by the occurrence of overall fracture, etc., so the intensity of the sound signal is higher.

4. Conclusions

In this study, we carried out grinding experiments on the whole life cycle of pyramid structure abrasive belts, explored the wear evolution law of the abrasive belts and its influence on the grinding process, and the results of the study can help to use this kind of abrasive belts in a better way. The main conclusions are as follows.

- (1) The main form of wear of pyramid-structured abrasive belts is abrasive wear, accompanied by adhesive wear and overall fracture of the abrasive cell, adhesive wear affects the cutting ability of the abrasive belts, so adhesive wear should be avoided as much as possible in the actual manufacture.
- (2) In the wear evolution of the pyramid-structured abrasive belts, the wear rate and material removal rate of the abrasive belts at the initial stage are at a high level and fluctuating, and with the increase of the grinding time, the first rapid decline, and then slowed down, and ultimately gradually lost the ability to polish the surface.
- (3) The machining performance of the pyramid-structured abrasive belts is relatively stable. Throughout their life cycle, before complete wear, the roughness values of the machined surfaces are stable at 0.4-0.5 μm for R_a and 0.1-0.2 μm for S_a . However, when the belts lose their ability to polish the surfaces, the roughness begins to deteriorate.
- (4) The worn state of a pyramid-structured abrasive belt affects the force and sound signals it

generates during the grinding process. With the deepening of the abrasive belt wear, the grinding tangential and normal forces tend to fluctuate and decrease, and the time-domain characteristics such as the RMS value of the sound signals show a tendency to change monotonically.

5. Contact Author Email Address

Wenxi Wang: wx.wang@cqu.edu.cn

6. Acknowledgments

This study was supported by the National Natural Science Foundation of China (52105430), China Postdoctoral Science Foundation (No. 2023M740398), and the Fundamental Research Funds for the Central Universities (No. 2023CDJXY-024).

7. Copyright Statement

The authors confirm that they, and/or their company or organization, hold copyright on all of the original material included in this paper. The authors also confirm that they have obtained permission, from the copyright holder of any third party material included in this paper, to publish it as part of their paper. The authors confirm that they give permission, or have obtained permission from the copyright holder of this paper, for the publication and distribution of this paper as part of the ICAS proceedings or as individual off-prints from the proceedings.

References

- [1] W. Wang, F. Salvatore and J. Rech. Characteristic assessment and analysis of residual stresses generated by dry belt finishing on hard turned AISI52100. *J. Manuf. Process.*, Vol. 59, pp 11–18, 2020.
- [2] G. Zhao, B. Zhao, W. Ding, L. Xin, Z. Nian, J. Peng, N. He and J. Xu. Nontraditional energy-assisted mechanical machining of difficult-to-cut materials and components in aerospace community: a comparative analysis. *Int. J. Extreme Manuf.*, Vol. 6, No. 2, pp 022007, 2024.
- [3] X. Xu, Z. Yang, Q. Liu, S. Yan and H. Ding. Condition monitoring and mechanism analysis of belt wear in robotic grinding of TC4 workpiece using acoustic emissions. *Mech. Syst. Signal Process.*, Vol. 188, pp 109979, 2023.
- [4] K. Zhou, G. Xiao, J. Xu and Y. Huang. Wear evolution of electroplated diamond abrasive belt and corresponding surface integrity of Inconel 718 during grinding. *Tribol. Int.*, Vol. 177, pp 107972, 2023.
- [5] Y. Huang, Y. Wu, G. Xiao, Y. Zhang and W. Wang. Analysis of abrasive belt wear effect on residual stress distribution on a grinding surface. *Wear*, Vol. 486–487, pp 204113, 2021.
- [6] H. Ding, J. Yang, W. Wang, Q. Liu, J. Guo and Z. Zhou. Wear mechanisms of abrasive wheel for rail facing grinding. *Wear*, Vol. 504–505, pp 204421, 2022.
- [7] Y. Cao, J. Yin, W. Ding and J. Xu. Alumina abrasive wheel wear in ultrasonic vibration-assisted creep-feed grinding of Inconel 718 nickel-based superalloy. *J. Mater. Process. Technol.*, Vol. 297, pp 117241, 2021.
- [8] Q. Wan, L. Zou, C. Han, W. Wang, K. Qian and J. Ou. A U-net-based intelligent approach for belt morphology quantification and wear monitoring. *J. Mater. Process. Technol.*, Vol. 306, pp 117652, 2022.
- [9] G. Xiao and Y. Huang. Experimental research and modelling of life-cycle material removal in belt finishing for titanium alloy. *J. Manuf. Process.*, Vol. 30, pp 255–267, 2017.
- [10] S. Mezghani, M. El Mansori and E. Sura. Wear mechanism maps for the belt finishing of steel and cast iron. *Wear*, Vol. 267, pp 86–91, 2009.
- [11] W. Wang, F. Salvatore, J. Rech and J. Li. Comprehensive investigation on mechanisms of dry belt grinding on AISI52100 hardened steel. *Tribol. Int.*, Vol. 121, pp 310–320, 2018.
- [12] Z. He, J. Li, Y. Liu and W. Wang. Investigation of conditions leading to critical transitions between abrasive belt wear modes for rail grinding. *Wear*, Vol. 484–485, pp 204048, 2021.
- [13] K. Serpin, S. Mezghani and M.E. Mansori. Multiscale assessment of structured coated abrasive grits in belt finishing process. *Wear*, Vol. 332–333, pp 780–787, 2015.
- [14] K. Serpin, S. Mezghani and M.E. Mansori. Wear study of structured coated belts in advanced abrasive belt finishing. *Surf. Coat. Technol.*, Vol. 284, pp 365–376, 2015.
- [15] S. Zaborski and W. Pszczółowski. Selected problems in evaluating topography of coated abrasives. *Arch. Civ. Mech. Eng.*, Vol. 6, pp 29–36, 2006.
- [16] G. Xiao, Y. Zhang, B. Zhu, H. Gao, Y. Huang and K. Zhou. Wear behavior of alumina abrasive belt and its effect on surface integrity of titanium alloy during conventional and creep-feed grinding. *Wear*, Vol. 514–515, pp 204581, 2023.
- [17] S. Song, G. Xiao, Y. Liu, K. Zhou, S. Liu and J. Huang. Tribological response of groove-textured surface with compressive stress on Ti6Al4V processed by laser and abrasive belt. *Tribol. Int.*, Vol. 180, pp 108265, 2023.
- [18] N. Wang, G. Zhang, L. Ren and Z. Yang. Analysis of abrasive grain size effect of abrasive belt on material removal performance of GCr15 bearing steel. *Tribol. Int.*, Vol. 171, pp 107536, 2022.
- [19] C. Cheng, J. Li, Y. Liu, M. Nie and W. Wang. An online belt wear monitoring method for abrasive belt grinding under varying grinding parameters. *J. Manuf. Process.*, Vol. 50, pp 80–89, 2020.
- [20] X. Zhang, H. Chen, J. Xu, X. Song, J. Wang and X. Chen. A novel sound-based belt condition monitoring method for robotic grinding using optimally pruned extreme learning machine. *J. Mater. Process. Technol.*, Vol. 260, pp 9–19, 2018.